Fluctuating optimum and temporally variable selection on breeding date in birds and mammals

Pierre de Villemereuil[1,2,29], Anne Charmantier[1], Debora Arlt[3], Pierre Bize[4], Patricia Brekke[5], Lyanne Brouwer[6,7,8], Andrew Cockburn[6], Steeve D. Côté[9], F. Stephen Dobson[10], Simon R. Evans[11,12], Marco Festa-Bianchet[13,6], Marlène Gamelon[14], Sandra Hamel[15], Johann Hegelbach[16], Kurt Jerstad[17], Bart Kempenaers[18], Loeske E.B. Kruuk[6], Jouko Kumpula[19], Thomas Kvalnes[14], Andrew G. McAdam[20], S. Eryn McFarlane[21,22], Michael B. Morrissey[23], Tomas Pärt[3], Josephine M. Pemberton[22], Anna Qvarnström[21], Ole-Wiggo Røstad[24], Julia Schroeder[25], Juan Carlos Senar[26], Ben C. Sheldon[11], Martijn van de Pol[7], Marcel E. Visser[7], Nathaniel T. Wheelwright[27], Jarle Tufto[28], and Luis-Miguel Chevin[1,29]

[1]CEFE, CNRS, Université de Montpellier, Université Paul Valéry Montpellier 3, EPHE, IRD, Montpellier, France; [2]Institut de Systématique, Évolution, Biodiversité (ISYEB), École Pratique des Hautes Études | PSL, MNHN, CNRS, Sorbonne Université, Université des Antilles, Paris, France; [3]Department of Ecology, Swedish University of Agricultural Sciences, Uppsala, Sweden; [4]School of Biological Sciences, University of Aberdeen, Aberdeen, UK; [5]Institute of Zoology, Zoological Society of London, Regents Park, London, UK; [6]Division of Ecology and Evolution, Research School of Biology, The Australian National University, Canberra, ACT 2600 Australia; [7]Department of Animal Ecology, Netherlands Institute of Ecology (NIOO-KNAW), Wageningen, The Netherlands; [8]Department of Animal Ecology and Physiology, Institute for Water and Wetland Research, Radboud University, Nijmegen, The Netherlands; [9]Département de biologie and Centre dÉtudes Nordiques (CEN), Université Laval, Québec G1V 0A6, Québec, Canada; [10]Department of Biological Sciences, Auburn University, Auburn, AL, 36849, USA; [11]Edward Grey Institute, Department of Zoology, University of Oxford, Oxford, OX1 3PS UK; [12]Centre for Ecology and Conservation, University of Exeter, Cornwall Campus, Penryn TR10 9FE, UK; [13]Département de biologie, Université de Sherbrooke, Sherbrooke, Québec, Canada; [14]Centre for Biodiversity Dynamics (CBD), Department of Biology, Norwegian University of Science and Technology, 7491 Trondheim, Norway; [15]Département de biologie, Université Laval, Québec G1V 0A6, Québec, Canada; [16]Institute of Evolutionary Biology and Environmental Studies, University of Zurich, Zurich, Switzerland; [17]Jerstad Viltforvaltning, Aurebekksveien 61, 4516 Mandal, Norway; [18]Department of Behavioural Ecology and Evolutionary Genetics, Max Planck Institute for Ornithology, Eberhard Gwinner Str, 82319 Seewiesen, Germany; [19]Natural Resources Institute Finland (LUKE), Terrestrial Population Dynamics, FIN-999870, Kaamanen, Inari, Finland; [20]Department of Ecology and Evolutionary Biology, University of Colorado, Boulder, USA; [21]Department of Ecology and Genetics, Uppsala University, Sweden; [22]Institute of Evolutionary Biology, School of Biological Sciences, University of Edinburgh, Edinburgh EH9 3FL, UK; [23]School of Biology, University of St Andrews, St Andrews, Fife KY16 9TH, UK; [24]Faculty of Environmental Sciences and Natural Resource Management, Norwegian University of Life Sciences, 1432 Ås, Norway; [25]Department of Life Sciences, Imperial College London, Silwood Park Campus, Ascot, UK; [26]Behavioural and Evolutionary Ecology Research Unit, Museu de Ciències Naturals de Barcelona, Barcelona, Spain; [27]Department of Biology, Bowdoin College, Brunswick, ME 04011, USA; [28]Centre for Biodiversity Dynamics (CBD), Dept of Mathematics, Norwegian University of Science and Technology (NTNU), NO7491 Trondheim, Norway

Temporal variation in natural selection is predicted to strongly impact the evolution and demography of natural populations, with consequences for the rate of adaptation, evolution of plasticity, and extinction risk. Most of the theory underlying these predictions assumes a moving optimum phenotype, with predictions expressed in terms of the temporal variance and autocorrelation of this optimum. However, empirical studies seldom estimate patterns of fluctuations of an optimum phenotype, precluding further progress in connecting theory with observations. To bridge this gap, we assess the evidence for temporal variation in selection on breeding date by modelling a fitness function with a fluctuating optimum, across 39 populations of 21 wild animals, one of the largest compilations of long-term datasets with individual measurements of trait and fitness components. We find compelling evidence for fluctuations in the fitness function, causing temporal variation in the magnitude, but not the direction of selection. However, fluctuations of the optimum phenotype need not directly translate into variation in selection gradients, because their impact can be buffered by partial tracking of the optimum by the mean phenotype. Analysing individuals that reproduce in consecutive years, we find that plastic changes track movements of the optimum phenotype across years, especially in birds species, reducing temporal variation in directional selection. This suggests that phenological plasticity has evolved to cope with fluctuations in the optimum, despite their currently modest contribution to variation in selection.

Adaptation | Fluctuating environment | Fitness landscape | Meta-analysis | Phenotypic plasticity

Introduction

Natural environments vary on multiple timescales, with consequences for the ecology and evolution of species in the wild (1–6). Beyond directional trends (e.g. global warming) and periodic cycles (diurnal, seasonal, pluriannual), most environmental variables exhibit random variation or noise (4, 6), the magnitude and temporal pattern of which are currently being altered by human activities (7, 8). From an evolutionary standpoint, these environmental fluctuations are important because they can lead to temporal variation in natural selection. This can in turn maintain genetic polymorphism and phenotypic/genetic variance of quantitative traits (9–12); select for traits that enhance evolvability (including the properties of mutations (13) or recombination (14, 15)); and favour the evolution of specific mechanisms to cope with environmental fluctuations, from (trans-generational) pheno-

Significance Statement

Many ecological and evolutionary processes strongly depend on the way natural selection varies over time. However, a gap remains when trying to connect theoretical predictions to empirical work on this question: most theory assumes that adaptation involves tracking a moving optimum phenotype through time, but this is seldom estimated empirically. Here, we have assembled a large database of wild bird and mammal populations, to estimate patterns of fluctuations in the optimum breeding date, and its influence on the variability of natural selection. We find that optimum fluctuations are prevalent. However, their influence on temporal variance in natural selection is partly buffered by tracking of the optimum phenotype through individual phenotypic plasticity.

typic plasticity to bet hedging (12, 16–18). A perpetually fluctuating environment also prevents natural populations from being perfectly adapted to their current conditions at any time, resulting in a "lag load" (19) that may impact population dynamics and extinction risk (20–23). Over macroevolutionary time, temporal variation in selection is also invoked to reconcile observations of rapid responses to selection with the relative paucity of long-term evolutionary change (6, 24–26).

Most theoretical work on adaptation to fluctuating environments rests on the classical framework of 'moving optimum models' (27), illustrated in Figure 1. In this model, directional selection on a quantitative trait is proportional to the deviation of the mean phenotype from an environment-specific optimum phenotype (Figure 1). Environmental fluctuations in the optimum phenotype can thus lead to temporal variation in directional selection, yet the two are not strictly equivalent, because changes in the expressed mean phenotype also affect temporal variation in deviations from the optimum, and thus in selection. A mean phenotype that closely tracks movements of the optimum (via evolution or phenotypic plasticity) can thus buffer the influence of a fluctuating optimum on selection (28, 29).

The wealth of theoretical predictions on adaptation to fluctuating environments (11, 12, 16–18, 20–22, 25) has rarely been explicitly compared to empirical estimates, especially for polygenic, quantitative traits, which form the bulk of ecologically important traits such as body size, behaviour or phenology (see Ref (6) for a review on fluctuating selection on discrete traits or major genes). Recent meta-analyses of temporal variation in selection on quantitative traits (30, 31) have shown that - when carefully restricted to datasets for which measurement error was reported (31) - the direction of selection was largely consistent across years, despite evidence for some temporal variation in magnitude of the gradients (31). However, neither of these meta-analyses (30, 31) allowed direct connection with theory, because most theoretical predictions are expressed in terms of the variance and autocorrelation in the optimum (11, 12, 16–18, 20–22, 25), which cannot be recovered directly from variation in selection gradients (as shown by ref. 29). In addition, these meta-analyses (30, 31) could not ascribe temporal variation in selection gradients to movements of the fitness function versus changes in the phenotype distribution (as illustrated in Figure 1).

Here, we investigate the extent of temporal variation in selection on breeding date. Breeding date can easily be compared across species, and is likely to be under selection for an optimum phenotype, because reproducing either too early or too late should limit reproductive success (including offspring survival), and possibly survival of the parents. Changes in phenology (the seasonal timing of life history events) are a predominant phenotypic response to climate change (32–35). Thus, understanding natural selection on phenology is crucial for many eco-evolutionary projections of the effects of current anthropogenic climate change on wild populations (36). In addition, most phenological traits (including breeding time) are plastic in response to environmental variables such as temperature, and this plasticity is thought to have evolved to buffer the ecological consequences of a moving optimum in a fluctuating environment (12, 16, 17, 37).

Instead of performing a meta-analysis of published selection estimates, we assembled a new database combining 39 long-term datasets from natural populations (13 bird and 8 mammal species, see Table S1), over periods spanning from 9 to 63 years. Although parts of these datasets have been published previously, we obtained up-to-date versions by directly contacting the PIs. This has allowed us to analyse temporal variation in natural selection using the common framework illustrated in Figure 1, using individual measurements of traits and fitness components. Based on key elements of the moving optimum theory of adaptation to a changing environment (27), we inquired: (i) Is there support for an optimum phenotype? (ii) Is there support for a temporally fluctuating fitness function? (iii) Does fluctuation of the fitness function translate into temporal variation in the direction and/or magnitude of selection? (iv) What is the predictability (autocorrelation) of selection? (v) To what extent is the effect of a moving optimum buffered by adaptive tracking by the mean phenotype, notably through phenotypic plasticity? While moving optimum models have previously been estimated in a couple of populations (38, 39), this is the first time that such a method has been applied systematically across a large number of populations and systems. This enabled us to report wild-population meta-estimates (robust overall estimators from "meta-analysis" models) of key parameters from the theory of selection in a variable environment.

Results

Selection model Consistent with moving optimum models (27), we assumed that the relationship between breeding date and the fitness component exerting selection on it (annual reproductive success) involves a single fitness peak, with an optimum phenotype that fluctuates with the environment (Figure 1). Denoting as $W(z)$ the expected fitness component for an individual with breeding date z, we thus have

$$W(z) = W_{\max} \exp\left(-\frac{(z-\theta)^2}{2\omega^2}\right), \qquad [1]$$

where θ is the optimum breeding date, for which the expected fitness component is $W_{\max}$, and ω describes the width of the fitness function. The fitness function in Equation 1, being quadratic on the log scale (38, 40), uses as many parameters as the quadratic approximation often used in selection analysis (30, 41–43), but is more realistic, notably because it precludes negative expected fitness (38, 40). This makes it a reasonable approximation for any fitness peak with an optimum (hence its prevalence in theoretical work (27, 44)), and a biologically meaningful benchmark to draw generalizations about temporal variation in selection across populations and species, even if it does perfectly match the actual fitness function for specific datasets (just like the effective population size allow comparing levels of drift even for non-Wright-Fisher populations).

In such a model, and assuming a normally distributed trait, the directional selection gradient measuring the strength of directional selection is (44)

$$\beta = \frac{\theta - \bar{z}}{\omega^2 + 1}, \qquad [2]$$

where $\bar{z}$ is the mean phenotype. Note that trait values are here divided by their standard deviation σ_z, so β corresponds to a standardised, dimensionless gradient (41), also described as selection intensity (θ and ω are similarly standardised; for
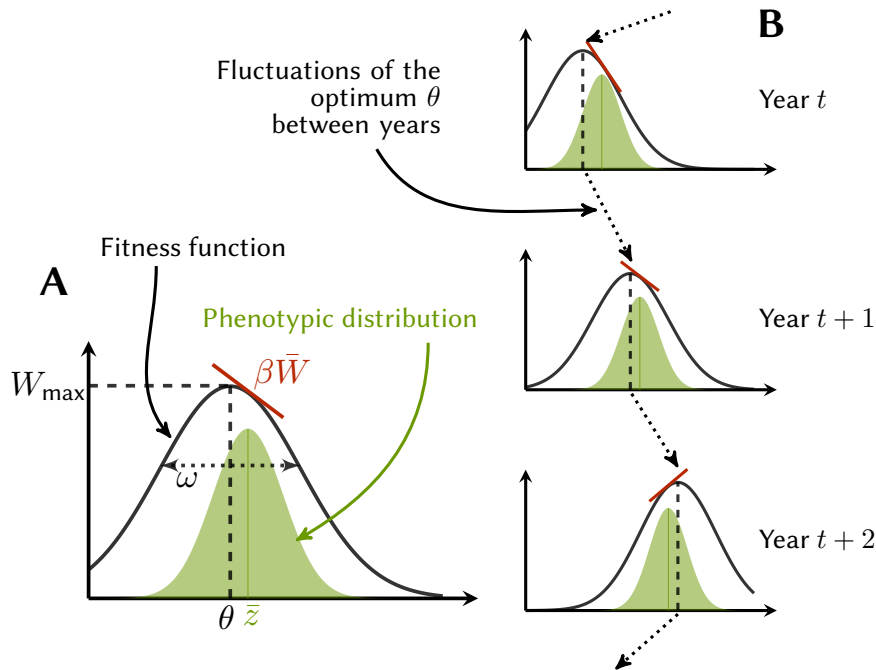
Fig. 1. **Selection in the moving optimum model.** **A**: A fitness peak with an optimum (black curve), is modeled as a Gaussian fitness function following classical theory of adaptation. The maximum absolute fitness W_{max} is reached at the optimal trait value θ, and the width of the fitness peak is parameterised by ω. A normal distribution of phenotypes is also shown underneath in green shading (note this distribution has its own scale of probability density, different from the fitness scale on the Y axis, but we omit it for simplicity). The strength of directional selection is quantified by the linear selection gradient beta, which measures the mean local slope of the relative fitness function, and is proportional to the slope of the red straight line. In this model of Gaussian fitness peak, β is proportional to the deviation of the mean phenotype from the optimum, and inversely proportional to $\omega^2 + 1$ (for SD-standardised traits), such that narrower fitness peaks cause stronger directional selection overall. **B**: Temporal changes in the optimum θ and in the mean phenotype (mode of the green distribution) jointly translate into changes in selection gradients β. Note that while the maximum fitness W_{max} remains constant in this figure, it is allowed to vary in our models.

a non-standardised trait, 1 should be replaced by σ_z^2 in Equation 2). Equation 2 shows that β is proportional to the deviation of the mean phenotype from the optimum, as illustrated in Figure 1. Fluctuations in directional selection (β) can thus result from fluctuations in the optimum phenotype (θ), fluctuations in the mean phenotype ($\bar{z}$), or both. Furthermore, fluctuations in the optimum might result in little to no fluctuations in directional selection, if the mean phenotype appropriately tracks changes in the optimum. For a given deviation from the optimum, β is larger if the fitness peak is narrower, leading to larger values of $1/(\omega^2 + 1)$. Note that the strength of stabilizing selection reducing phenotypic variance in any generation is also proportional to $1/(\omega^2 + 1)$ (or $1/(\omega^2 + \sigma_z^2)$ for an unstandardised trait), regardless of the deviation of the mean phenotype from the optimum (45, 46), such that the trait can be under both stabilizing and directional selection.

We are interested in distinguishing temporal variation in selection caused by fluctuation in the fitness function from that caused by changes in the mean phenotype (Figure 1). To this aim, we directly estimated fluctuations of the fitness peak via a random effect for year t on the optimum θ_t in a mixed model, which prevents conflating measurement error with the actual variance in selection (38, 39). We also investigated the temporal predictability of fluctuations in the optimum, by optionally allowing for temporal autocorrelation in the optimum, in the form of a first-order autoregressive process. As alternative models, we also considered fitness functions without an optimum, namely a monotonic fitness function where the direction of selection does not change with the mean phenotype in the population (but can still change with the environment), and a flat fitness function causing no selection. The models are summarised in Table 1.

Fluctuation of the fitness function is predominant We first investigated the support for fluctuating fitness functions, by using

an information criteria akin to AIC or WAIC, the Bayesian Leave-One-Out Information Criterion (47) (LOOIC). More specifically, we computed "weights of evidence" inspired by Akaike weights used in model averaging (48) (and summing to 1 across all compared models), which we used to compare the statistical support for different features of selection across datasets. The results of model selection for each dataset appear in Table S2. We found little support for models without selection (flat fitness function, 3.4% and 8%, respectively for birds and mammals). The statistical support for an optimum was dominant (optimum vs directional models: 51.7% vs 44.9% for birds and 62.4% vs 29.6% for mammals). Similarly, the support for fluctuating fitness functions was also dominant (fluctuating vs constant models: 77.7% vs 22.3% for birds and 65.6% vs 34.4% for mammals). Those results were qualitatively unchanged when considering a completely balanced setting using ConstDir/ConstOpt models as the sole contestants for "no fluctuation" and FluctCorrDir/FluctCorrOpt as the sole contestants for "fluctuating fitness functions". For some datasets, especially the smaller ones and/or those where fitness was analysed as a binary trait, there was considerable uncertainty regarding the best model(s), even when there was clear evidence for fluctuating fitness functions. For two datasets, the mountain goat (*Oreamnos americanus*, Oam) and the red-winged fairy-wren (*Malurus elegans*, Mel), the support for an absence of selection was dominant (weight above 0.5), so we removed them from subsequent analyses to avoid commenting on spurious signals. In the rest of the paper, and for the sake of simplicity, we focus on the (maximal) model with an auto-correlated fluctuating optimum, unless otherwise noted. However, we also discuss the support for different aspects of the model when commenting on the results.

The optimum fluctuates differently between birds and mammals In datasets with predominant support for an optimum (rel-

Table 1. Statistical models considered, their characteristics and relative statistical support for each taxonomic level (birds, 31 datasets, or mammals, 8 datasets, or all taxa together, 39 datasets). "NoSel" corresponds to a flat fitness function, i.e. no selection. "Const" models have a constant fitness function, "Fluct" models have fluctuating optimum without correlation between years, while "FluctCorr" models have auto-correlated fluctuating optimum. In all models, the intercept was allowed to vary from year to year. Regarding the shape, "Dir" models correspond to a monotonic (directional) function, while "Opt" models include an optimum as described in Figure 1 and Equation 1. Relative statistical support is the average of the evidence weights (computed from Leave-One-Out information criterion, LOOIC(47), following (48)) over the total number of tested models (note that relative statistical supports sum up to 1).

ID	Shape	Fluctuations	Autocorrelation	Statistical Support		
				Bird	Mammal	Total
NoSel	Flat	✗	✗	0.034	0.08	0.043
ConstDir	Monotonic	✗	✗	0.12	0.082	0.112
ConstOpt	Gaussian	✗	✗	0.069	0.182	0.092
FluctDir	Monotonic	✔	✗	0.188	0.104	0.171
FluctOpt	Gaussian	✔	✗	0.194	0.211	0.198
FluctCorrDir	Monotonic	✔	✔	0.141	0.11	0.135
FluctCorrOpt	Gaussian	✔	✔	0.254	0.231	0.249

ative support >0.5 among models with selection), the peak width ω was typically large (Figure S1 and Figure S2), with a meta-estimate of 6.22 (95% higher posterior density credible interval [3.2, 9.4]) for birds and of 4.94 ([1.2, 9.2]) for mammals. Such values (in units of within-year phenotypic SD) correspond to weak stabilising selection (fitness peak broader than phenotype distribution), consistent with previous estimates from the literature, and with values commonly used in theory (42, 43, 49). A few notable exceptions had a narrow fitness peak with a low value of ω (e.g. an Alpine swift dataset, *Tachymarptis melba*, Tme1; the eastern grey kangaroo, *Macropus giganteus*, Mgi; the oystercatcher, *Haematopus ostralegus*, Hos; and the reindeer, *Rangifer tarandus*, Rta). The lowest ω was found in the hihi (*Notiomystis cincta*, Nci, 1.77 [1.56, 2.03]).

The mean location of the optimum θ_t was often inferred to be significantly negative, implying that the average optimal timing was usually earlier than the average mean breeding date across years (Figure 2). In the three cases when a point estimate was inferred to be positive, the sign of the estimate was uncertain (i.e. 95% credible intervals overlap zero), despite strong support for a model with an optimum for one of them (a blue tit, *Cyanistes caeruleus*, Cca10). The meta-estimate for birds was different from zero (-3.7, $[-7.5, -0.7]$), while that for mammals was not (-1.75, $[-6.4, 3.0]$, Figure 2).

The magnitude of fluctuations in the optimum differed strongly between datasets, with five datasets (out of twenty with predominant support for an optimum) displaying low variation ($\sigma_\theta < 0.5$, Figure 2) and five inferred to have a large standard deviation ($\sigma_\theta > 3$, Figure 2). Note that the latter also had $E(\theta)$ not significantly different from zero, which could be linked to a greater uncertainty in the estimation of $E(\theta)$ in the context of high levels of fluctuations. The meta-estimate for σ_θ was higher for mammals (3.14, [0.34, 6.7]) than for birds (1.89, [0.33, 4.1], Figure 2). Interestingly, there was no obvious link between statistical support for fluctuations and the inferred standard deviation of the optimum (orange scale in Figure 2). Autocorrelation of the optimum was difficult to estimate, resulting in large 95% credible intervals overlapping zero most of the time (φ in the left panel of Figure S1 and Figure S2). Still, six datasets had a significant estimate of temporal autocorrelation in the optimum, of which five were positive (blue tits, Cca7: 0.59[0.31, 0.84],

CCa9: 0.42 [5.9×10^{-4}, 0.80], Cca10: 0.94 [0.84, 0.99] and great tits, *Parus major*, Pma4: 0.74 [0.42, 0.97] and Pma8: 0.83 [0.64, 0.97], all from the Netherlands except Pma8). The only dataset with a significantly negative temporal autocorrelation was the hihi (Nci, $-0.59[-0.98, -0.097]$). Overall, these differences between datasets resulted in a wide variation across datasets of the behaviour of the fitness function over years (Figure S3).

Selection varies in strength, but not in direction The inferred selection gradients β_t were consistent between models with and without an optimum (computed following (40, 50)) for the same dataset (Figure S4), so we hereafter only focus on results from the model with an optimum to avoid over-fitting resulting from model selection.

The temporal mean of the standardised selection gradient $E(\beta)$ was significantly negative (selection for earlier breeding) for most bird datasets (only three great tit datasets, Pma2, Pma3 and Pma5 were not significantly negative; and one, a blue tit dataset, Cca10, was significantly positive, Figure 2). On the contrary, the temporal mean gradients for mammals were mostly not significant (with two exceptions, the reindeer, Rta and the Columbian ground squirrel, *Urocitellus columbianus*, Uco, Figure 2). The meta-estimates for the temporal mean of standardised gradient reflected these individual results, being significantly negative for birds (-0.17, $[-0.26, -0.077]$) but not for mammals (-0.087, $[-0.22, 0.032]$, Figure 2). Six datasets (the European oystercatcher, Hos; eastern grey kangaroo, Mgi; hihi, Nci; the reindeer, Rta; and two Alpine swift datasets, Tme1 and Tme2) had stronger mean selection gradients than the others (Figure 2). Interestingly, large mean selection gradients over years (large absolute values of $E(\beta)$) were sometimes associated with predominant support for an optimum, and were then attributable to a narrow fitness peak (small ω) rather than to a large temporal mean deviation from the optimum (large $E(\theta)$, Figure S5).

The magnitude of variation in directional selection, as quantified by σ_β, was highly different between datasets, although less so than for σ_θ. Overall, variation in standardised gradients ranged from very small to large (0.004 to 0.38 for the posterior medians of σ_β), with meta-estimates at 0.047 ([0.018, 0.11]) for birds and 0.15 ([0.056, 0.36]) for mammals (Figure 2). Despite such possibly large variation, there was very little evidence for fluctuations in the sign of selection gra-
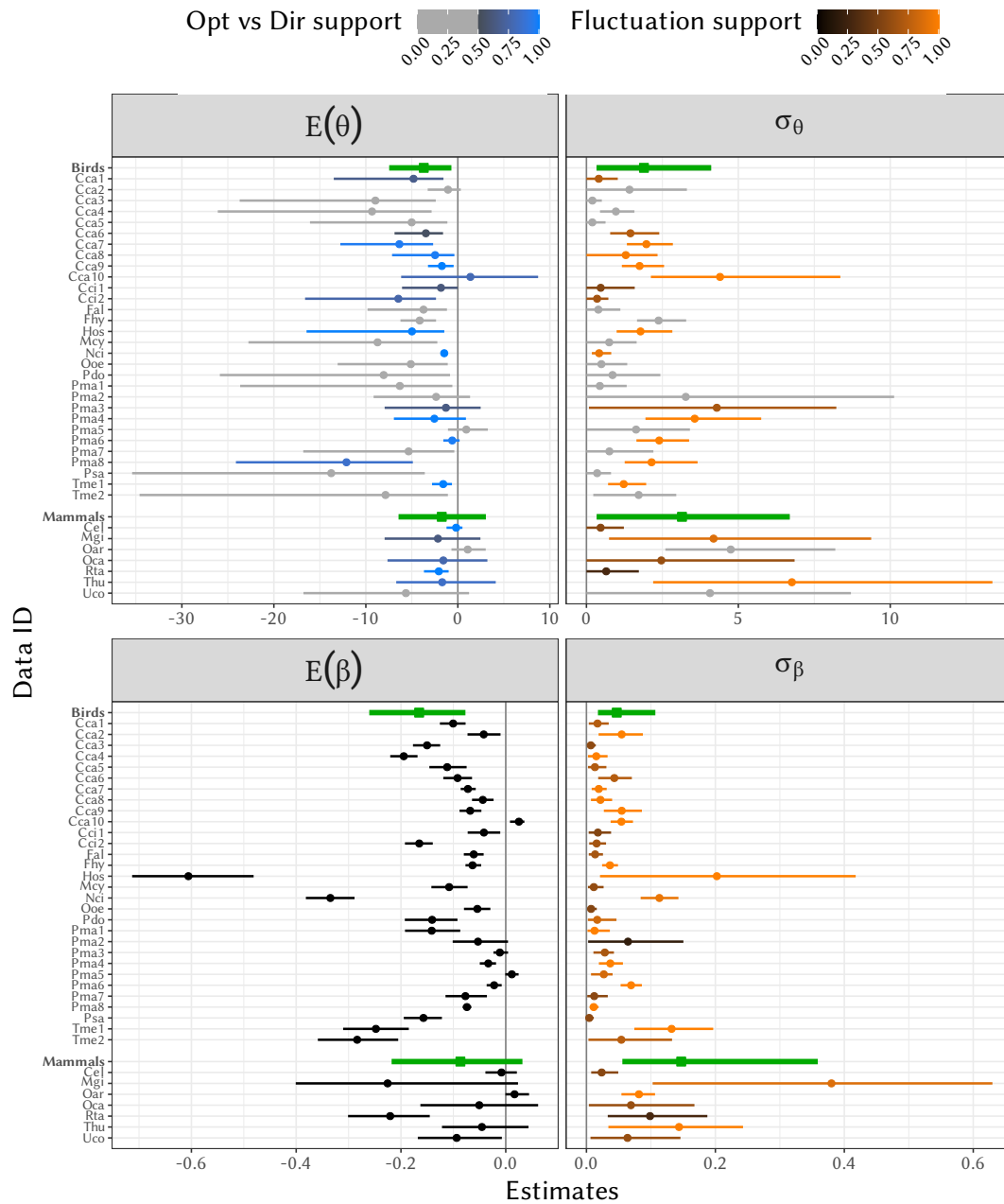
Fig. 2. Strength and variation of selection. The average location of the optimum $E(\theta)$ (top left, where 0 represents the mean breeding time across years) and selection gradients $E(\beta)$ (bottom left) are shown, together with their temporal standard deviations σ_θ (top right) and σ_β (bottom right), for all datasets (points: posterior median, lines: 95% credible intervals). Meta-estimators for birds and mammals (computed on datasets with majority optimum support for the top panels) are available at the bottom of each panel (in green, with squares and thicker lines). Note that the phenotypes were mean-centred and scaled to a within-year variance of 1, so θ and β are dimensionless. The evidence weight for an optimum (vs directional models, excluding NoSel models) phenotype is indicated by a colour on the blue scale on the top-left panel, while the orange scale on the right panels represents the evidence weight for fluctuating selection (more saturated colours for higher values, i.e. more support for the estimate). Datasets for which the optimum support was in minority (< 0.5) compared to directional models are greyed out in the top panels. Estimates computed from FluctCorrOpt models. The dataset codes are explained in Table S1 and the values are provided in a CSV file on the GitHub repository.

dients (e.g. negative gradients becoming positive, Figure S6, 49% of datasets with strong support for no change of sign at all), and such fluctuations were more frequent (posterior median above 30%) for datasets with an especially small average gradient ($-0.04 < E(\beta) < 0.02$). Again, there was no link between statistical support in favour of fluctuations and the inferred σ_β (Figure 2, levels of orange), which suggests that moderate variation in selection could still be strongly

supported by the data.

Plasticity causes adaptive tracking of the optimum phenotype To better understand the causes of variation in directional selection, we disentangled the relative contributions of fluctuations in the optimum phenotype *vs* in the mean phenotype (Figure 1). From Equation 2, the variance of selection gradients

de Villemereuil *et al.*

PNAS | **September 30, 2020** | vol. XXX | no. XX | **5**
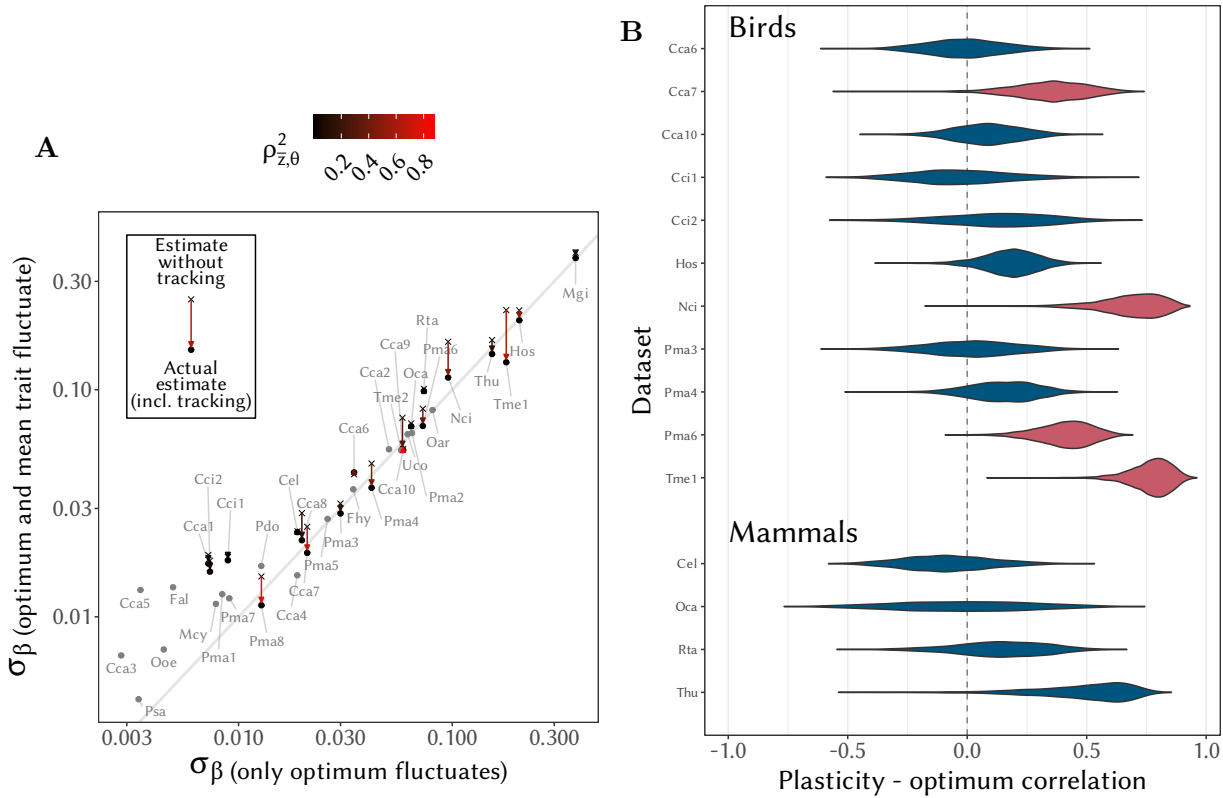
Fig. 3. Phenotypic tracking of fluctuations in the optimum. **A**: Standard deviation of the selection gradient β_t (dots: actual values σ_β; crosses: computation assuming no tracking, i.e. $\rho_{\bar{z},\theta} = 0$ in Equation 3) against the standard deviation expected when using optimum fluctuations only (i.e. $\sigma_{\bar{z}} = 0$ in Equation 3). Arrows show the direction of the change when accounting for tracking, and the red scale indicates the actual value of $\rho_{\bar{z},\theta}^2$. Note that long arrows tend to be red, while short arrows tend to be grey. For datasets with minority support for an optimum compared to the directional models, only greyed-out dots are displayed. The identity line is depicted in grey. **B**: For the 15 datasets with predominant support for an optimum and repeated measures, posterior distributions (coming from propagated Bayesian uncertainty) of the correlation coefficients between shifts in the optimum and shifts in the average phenology for individuals measured in two consecutive years. In light red: the distribution does not contain zero in the 95% highest density posterior interval. The dataset codes are explained in Table S1.

is

$$\sigma_\beta^2 = \frac{\sigma_\theta^2 + \sigma_{\bar{z}}^2 - 2\rho_{\bar{z},\theta}\sigma_\theta\sigma_{\bar{z}}}{(\omega^2 + 1)}. \qquad [3]$$

Equation 3 shows that the temporal variance in directional selection gradients σ_β^2 results not only from fluctuations in the optimum, with variance σ_θ^2, but also from year-to-year fluctuations in the annual mean phenotype $\bar{z}$, with variance $\sigma_{\bar{z}}^2$. Fluctuations in $\bar{z}_t$ are explained by a combination of phenotypic plasticity (adaptive or not), responses to selection, and drift (neglecting the influence of dispersal). In addition, σ_β^2 depends on the correlation $\rho_{\bar{z},\theta}$ between the mean phenotype and the optimum (hereafter referred to as phenotypic tracking of the optimum). A positive $\rho_{\bar{z},\theta}$ is indicative of adaptive change in the mean phenotype, as produced by adaptive phenotypic plasticity and/or genetic responses to natural selection.

The dots in Figure 3A show the estimated standard deviations of selection gradients σ_β, plotted against their hypothetical values if we solely include fluctuations in the optimum, by assuming $\sigma_{\bar{z}} = 0$ in the numerator of Equation 3. Even for datasets with moderate or weak support for an optimum (grey dots), fluctuations of the optimum are a very good predictor of variation in selection gradients, as the points are close to the identity line (in light grey, which corresponds to the assumption that all variance in β originates from variance in the

optimum θ). In cases where the optimum causes little variation in β (bottom left), the actual σ_β was inflated relative to this identity line. This inflation originates from mild fluctuations in the mean phenotype (with magnitude $\sigma_{\bar{z}}$), which become non-negligible relative to small values of σ_θ, and therefore contribute to variation in deviations from the optimum. The crosses in Figure 3A show, for datasets with predominant support for an optimum, the hypothetical standard deviations of selection gradients in the absence of phenotypic tracking of the optimum, that is, keeping only $\sigma_{\bar{z}}^2$ and σ_θ^2 in the numerator of Equation 3, while setting $\rho_{\bar{z},\theta} = 0$. The arrows connecting crosses to dots thus represent the influence of phenotypic tracking on variation in selection gradients: the longer the arrow, the more $\rho_{\bar{z},\theta}$ becomes important to understand σ_β (Equation 3). These arrows are pointing down in most cases, indicating that realised σ_β were smaller than expected when assuming independent fluctuations in the optimum and mean phenotype. The length of the downward facing arrows can thus be interpreted as the degree to which temporal variation in selection was reduced by phenotypic tracking of the optimum causing a positive $\rho_{\bar{z},\theta}$ (colour of the arrows in Figure 3).

An obvious candidate mechanism for phenotypic tracking of the optimum is adaptive phenotypic plasticity (51, 52). Using only individuals with repeated measures in subsequent years (on a subset of 15 datasets with both predominant sup-

de Villemereuil *et al.*

port for an optimum and sufficient repeated-individual data), we were able to distinguish plastic from genetic changes in mean breeding date. We detected plastic phenotypic tracking of fluctuations in the optimum (Figure 3B), especially in four datasets for which the correlation between plastic phenotypic change and change in the optimum was significantly positive (in red in Figure 3B; note that Cca7 and Pma6 are both located in Hoge Veluwe in the Netherlands). The meta-estimate of the correlation across the 11 bird datasets was relatively strong and significant for birds $(0.25 [0.072, 0.44]$, $p = 0.0095)$, contrary to the meta-estimate across the 4 mammal datasets $(0.13 [-0.17, 0.43]; p = 0.35)$. Note however that American red squirrel (*Tamiasciurus hudsonicus*, Thu) had a large correlation (0.53), which despite being non-significant using sample-based *p*-value $(p = 0.0675)$, had a 95% higher posterior density interval non-overlapping zero $([0.056, 0.78])$. These results suggest that phenotypic plasticity indeed plays an important role in tracking the optimum phenotype, at least in bird species.

Discussion

We investigated fluctuations of fitness functions and temporal variation in selection, as estimated by the relationship between individual breeding date and yearly reproductive output. Our unique database, comprising 39 datasets of wild populations of birds and mammals, allowed for an unprecedented estimation of parameters that appear in a wealth of theoretical predictions for adaptation to changing environments (11, 12, 16–18, 20–22, 25), answering our key questions laid out in the Introduction. In summary, we found predominant support for *(i)* models with a fitness peak against the alternatives and *(ii)* fluctuations of the fitness function over time. This translated into *(iii)* variation in the strength but not direction of selection, with a strong dependence on taxa (mammal/bird), species and population. We found *(iv)* uncertainty in the estimation of autocorrelation in the optimum and directional selection, owing to the high data requirements of these estimates. But we showed *(v)* substantial plastic phenotypic tracking of the optimum phenotype between years for bird species. Beyond our case study on reproductive phenology, the range of parameters we estimated here can serve as a much-needed benchmark of biologically realistic values for theoretical studies of adaptation to changing and fluctuating environments.

Our results corroborate a consensus in the bird literature that natural selection on phenology tends to favour earlier breeding (35), with a significantly negative meta-estimate for the directional selection gradients (Figure 2). This pattern, which has been documented before (35, 39, 51, 53–60), was however not found in mammals overall, despite two individually significant datasets (Figure 2), previously shown to be under such negative selection (61, 62). We also found support for the presence of an optimum phenotype (total statistical support of 54% for models with an optimum, Table 1), with slightly more support in mammals, perhaps in relation to the difference in significance of the selection gradient above. Support for an optimum is consistent with the intuition that breeding too early or too late should be detrimental in the temperate locations constituting most of our database, characterised by marked seasonality with stressful conditions in winter and summer (61, 62). This raises the question, espe-

cially for birds: why are breeding dates in these populations not closer to their expected evolutionary equilibrium, instead displaying consistent deviations from their optimum? Among several possible explanations for this "paradox of stasis" (63), a particularly relevant one for breeding time involves body condition (64). Non-heritable aspects of physiological condition (e.g. nutritional status) are known to influence both the timing of breeding and reproductive output, such that individuals in better condition tend to breed earlier and have more offspring (64). This causes the optimal breeding date to be displaced to a later time than the optimum set by the external environment (e.g. date of peak in resource abundance), such that apparent directional selection - mediated by condition - persists even at evolutionary equilibrium (64). Another mechanism with a similar outcome is when competition for breeding territories produces frequency-dependent selection favoring individuals that breed earlier than others in the population, regardless of the actual date (65). In that light, the difference between birds and mammals, in both the significance of mean selection gradients and support for an optimum, could stem from differences in how inter-individual competition is happening over time, with possibly shorter periods of stronger competition when birds feed the chicks. Note that temporal variation in condition, or in its relationship with breeding date and reproductive success, could also contribute to the estimated variation in selection to some extent. A promising approach for partitioning out this effect would be to include a proxy for physiological condition in a multivariate selection analysis. More broadly speaking, trade-offs with other components of fitness not included in our estimate of selection, such as maternal survival or future performance (66), could also affect our inference of natural selection and its variation.

Our analysis indicates that the strength of natural selection on a phenological trait, one of the best studied phenotypic categories in evolutionary ecology, varies in time in most investigated wild populations of birds and mammals (Figure 2). Models including variation in the strength of selection and/or fluctuations of an optimum phenotype had statistical support above 75% (all taxa together, Table 1), and the standard deviation of standardised selection gradients was relatively large, up to 0.38. However, we found little variation in the *direction* of selection, consistent with findings of a previous study based on a meta-analysis (31). Nevertheless, theoretical work has shown that randomly varying selection can have substantial eco-evolutionary impacts, even when the direction of selection does not fluctuate. Indeed, environmental stochasticity causes randomness in evolutionary trajectories, increasing both the average magnitude and stochastic variance of phenotypic mismatches with optimum, in turn leading to higher extinction probability in a novel or changing environment (20–22). These studies have shown that the demographic load (expressed as a reduction in log mean fitness) caused by a fluctuating optimum is proportional to $\frac{\sigma_\theta^2}{2(\omega^2+1)}$ (for a SD-standardised trait), which we here estimate as 0.199 $([1.6 \times 10^{-5}, 0.99])$ for birds and 0.401 $([0.0067, 1.6])$ for mammals, equivalent to a 18% (respectively 33%) decrease in mean fitness.

Environmental fluctuations might not result in detectable variation in natural selection if populations track their fluctuating optimum over time. In datasets for which an opti-

mum was well supported, we found that fluctuations in the optimum strongly influenced temporal variation in selection gradients (Figure 3A), but that the latter was considerably attenuated by phenotypic tracking of the optimum. We demonstrated that this phenotypic tracking is largely caused by plastic responses of individuals that reproduce in consecutive years (Figure 3B), with four datasets showing a significant correlation (from 0.36 to 0.78) between changes in the optimum and plastic change in the mean phenotype. A significant meta-estimate of this correlation was found for birds (no perfect tracking —correlation of 1— was detected, as would be expected(67)). The meta-estimate was not significant for the tested mammal datasets, which were mainly ungulates. Although difficult to generalise based on only four datasets, it is possible that because in mammals gestation periods are often longer than for birds and annual fitness is often measured based on offspring recruitment (Table S1), tracking selection through plasticity might be particularly challenging for mammals. An exception to this trend was the only non-ungulate (American red squirrel, Thu), for which tracking was partially supported, consistent with previous findings in this species (23). It is possible that the natural history of this species —food hoarding (68) and year-round social cues of density (69)— provides access to cues of upcoming natural selection that are typically not available to other species.

Even when plastic phenotypic tracking was strong, the mean breeding time was consistently late relative to the optimum, thus questioning the adaptiveness of plasticity in these populations. Given that environmental cues strongly associated with phenological plasticity have been detected in all of the populations with substantial support for plastic tracking (60, 70–72), it is likely that such cues allow tracking of the optimum, but are somehow biased toward later phenology. A possible reason may be that the mean phenology is lagging behind an advancing optimum caused by warming climate, and that the reaction norm for plasticity is shallower than that for the optimum (67, 73). For example, the significant positive autocorrelation signal observed in five of our datasets can be explained by a significant trend over years (without much impact on the estimate of σ_θ for all five, but resulting in non-significant autocorrelation in two cases, see Figure S7). Another possibility is that cue reliability has been reduced under climate change and habitat degradation, causing originally adaptive phenotypic plasticity to become less suitable for tracking the optimum phenotype. This scenario, which is predicted to cause evolution of the environmental cues used by organisms to plastically adjust their phenotypes (74), remains to be investigated further.

Material & Methods

Data collection. We assembled a collection of surveys of wild populations for which episodes of fertility selection on reproductive phenology were monitored over multiple years, allowing estimation of parameters of fluctuating selection. To enter the database, a dataset had to include information on both (i) a trait relating to reproductive phenology, such as lay or parturition date; and (ii) a measure of fitness for this selection episode, such as number of viable offspring or survival of offspring, which quantify the output of a reproductive event. We also only retained datasets with a sufficiently large number of years (at least nine years). The final collected database includes $N_d = 39$ datasets, with 21 different species (13 birds and 8 mammals) and 32 different locations. The number of years varied between 9 and 63 (average 33.2) and the average number of females breeding per year between 15.7 and 236.3 (average 64.8) for a total of between 353 and 12357 breeding events (average 1880). More detailed information on each dataset is available in Table S1.

Data formatting. All datasets were formatted consistently. In case of multiple breeding events per breeding season, we used the date of the first event as the phenological trait (onset of breeding); otherwise, we used the start date of the unique breeding event. For each dataset, this phenological trait was centred to the overall mean across years for the dataset and standardised by dividing by the average within-year phenotypic standard deviation, also for the dataset. As a measure of reproductive output for each female and breeding event, we used the number of fledglings summed over the entire breeding season for bird species, and the number of offspring at weaning, or alive after a year, for mammals with large numbers of offspring. For mammals with one (occasionally two) offspring

per breeding event, we used the survival to weaning or to a year after birth. Whether a data set was using weaning or the one-year threshold as the reference was decided in agreement with the contributors and is shown in Table S1. All records with a missing value for either the phenological trait or the fitness measure were removed. A dummy ID was assigned for each record missing a female ID.

Statistical analyses.

Fitness function Expanding on (38), we contrasted three shapes of the fitness function relating the phenological trait to fitness in each breeding season: *(i)* a flat function corresponding to no selection ("NoSel" model); *(ii)* a monotonic function for which the direction of selection is independent of the mean phenotype ("Dir" models); and *(iii)* a Gaussian optimum ("Opt" models). Denoting as $W(z)$ the expected number of offspring of an individual with phenotype z, these fitness functions took the following mathematical forms when fitness consisted of a count of offspring:

$$(i) \qquad W(z) = \exp(a), \qquad [4a]$$

$$(ii) \qquad W(z) = \exp(a + bz), \qquad [4b]$$

$$(iii) \qquad W(z) = W_{\max} \exp\left(-\frac{(z-\theta)^2}{2\omega^2}\right). \qquad [4c]$$

Note that for the exponential fitness function in *(ii)*, the directional selection gradient is the parameter b (40), regardless of the phenotype distribution. For the Gaussian fitness peak in *(iii)*, the parameter ω describes the width of the fitness function, with smaller ω causing stronger stabilising selection, while θ is the optimal timing for reproduction, and directional selection depends on the mean deviation from the optimum, as illustrated in Figure 1. Since the phenological traits were standardised, θ and ω are in units of within-year phenotypic standard deviation. When fitness measures consisted of survival of one offspring, we replaced the exponential in *(i)* and *(ii)* with an inverse-logit, while for *(iii)* we retained the Gaussian fitness peak in Equation 4c, but obtained $W_{\max} \in [0, 1]$ from a continuous latent scale on real numbers via a logit link. The realised reproductive output was then obtained from this expected fitness using a Poisson or binomial distribution, depending on whether the fitness measures were a number or individual survival of offspring, respectively. The Poisson distribution could further be zero-truncated or zero-inflated, if posterior predictive checks on a Poisson model were showing a bad fit for the zero category. Furthermore, we included female IDs as a random effect on the intercept (a in *(i)* and *(ii)* and $W_{\max}$ in *(iii)*), to account for repeated measurements.

Models of fluctuating selection To investigate temporally variable selection ("Fluct" models throughout, e.g. "FluctOpt" and "FluctDir"), we allowed the fitness function to vary from year to year, using random effects for time in the relevant parameters (see below), as in (38, 39). For models with an optimum, a random effect for year was included for both $W_{\max}$ and θ (on the log or logit scale for $W_{\max}$). We did not allow ω to vary between years, because it is a difficult parameter to infer, and within-year sample sizes were likely not enough to bear with its estimation for each year. We can thus think of our estimates as fluctuations of an effective optimum with constant width, even though the true optimum may vary in

width to some extent. For models without an optimum, we used random effects for years on the a and b parameters. The random effects (following a Gaussian distribution) allowed us to infer the standard deviation over years of θ and $W_{\max}$ (on the log or logit scale), σ_θ and $\sigma_{W_{\max}}$, and of a and b, σ_a and σ_b. Models with only variation in the intercept ($W_{\max}$ or a) are referred to as "Const" models, because although the function varies in intercept from year to year, the actual *selection* process is assumed constant. Temporal autocorrelation, in the form of a first-order auto-regressive process (AR1) with slope φ, was optionally introduced in the random effects for the θ and b parameters (referred to as "FluctCorr" models).

The combination of fitness functions and patterns of fluctuations led to seven alternative parameterisations, which are summarised in Table 1. To compare the magnitude of selection and its fluctuation across models with alternative fitness functions, we computed the selection gradients β_t (estimated for each year t if fluctuations are assumed) from both kinds of statistical models with selection. For models with monotonic directional selection (ConstDir, FluctDir, FluctCorrDir), the selection gradient is simply the slope of the linear model $\beta_t = b_t$ when using the log-link, and was computed for logit-link as:

$$\beta_t = b_t \left(1 - \frac{\overline{W_t^2}}{\overline{W_t}}\right), \qquad [5]$$

where $\overline{W_t}$ and $\overline{W_t^2}$ are respectively the population mean fitness and mean squared fitness, computed over all available individuals each year, adapted from (50). For models including an optimum, the directional selection gradient in year t is as in Equation 2. Note that with an optimum, variation in directional selection gradients must account for year-to-year variation in the mean phenotype $\bar{z}_t$ (Figure 1).

Prior distributions Diffuse, zero-centered normal distributions (with variance 10^6) were chosen as priors for $\log(W_{\max})$, θ, a and b, while for $\text{logit}(W_{\max})$ in the binomial model, we used a weakly informative normal distribution with mean 0 and standard deviation of 1. In contrast, we used a slightly informed prior for ω, because we do not expect the fitness peak to be narrow relative to the phenotypic standard deviation, since this would lead to extremely strong stabilising selection, with most phenotypes having a fitness near zero, except in the immediate vicinity of the optimal timing for reproduction. We thus used a Gamma distribution parameterised so that 95% of the prior distribution lies between 1 and 10 standard deviations of the trait (standardised to 1), leading to a shape parameter of 3.36 and a rate parameter of 0.78. The variances of the random effects added to $\log(W_{\max})$, a and b were assigned a weakly informative standard normal distribution prior, while the prior variance of σ_θ was specified indirectly via an independent exponential prior of rate 1 on $c = \sigma_\theta/\omega$. Finally, the zero-inflation probability p_{zi} was assigned a uniform prior between 0 and 1, and the auto-regressive coefficient φ a uniform prior between -1 and 1.

Statistical implementation We implemented the models using Hamiltonian Monte Carlo (HMC) as available in the Stan framework (75). We ran 10 chains, each with 2000 iterations following a burn-in of 1000 iterations. After a thinning every 5 iterations, we obtained a total of 4000 iterations. Divergent

de Villemereuil *et al.*

PNAS | **September 30, 2020** | vol. XXX | no. XX | **9**

transitions can happen during HMC and hamper safe interpretation of the output. Given the high number of models to be analysed, we kept models with divergent transitions, though only if at low rates (less than 2.5% of the iterations), increasing the adapt_delta parameter in Stan as needed to reach this threshold. Convergence was checked graphically, and using the potential scale reduction factor diagnostic (76). Effective sample size was kept above 200 for all parameters.

Model selection The models were compared using a cross-validation procedure, namely approximate leave-one-out with Pareto smooth importance sampling (47) (LOO-PSIS). An information criterion can be derived from LOO-PSIS, named LOOIC, which was used to compare models. LOOIC is akin to WAIC (but does not rely on asymptotic assumptions(47)), and can be interpreted in a similar fashion as other information criteria such as AIC or BIC. In order to compute the overall statistical support, across datasets, for each model in Table 1, we derived "weights of evidence" inspired by Akaike weights used in model averaging (48), but based on LOOIC. The relative support for model i across datasets was defined as

$$w_i = \frac{1}{N_d} \sum_{j=1}^{N_d} \frac{\exp(-\Delta_{i,j}/2)}{\sum_{k=1}^{7} \exp(-\Delta_{k,j}/2)}, \qquad [6]$$

where $\Delta_{i,j}$ is the difference between the LOOIC of the best model and that of the focal model i (k iterates over the seven models), both for dataset j, and N_d is the total number of datasets as defined above. We repeated the same analysis using only birds and then only mammals datasets, adjusting N_d in Equation 6 as needed.

This procedure of using weights of evidence was preferred over a simple computation of the proportion of datasets for which each model was the best model because the latter would necessarily be less precise. For instance, when several models (say, all those with fluctuating selection) have very similar LOOIC scores, but differ substantially from the remainder of the models for a given dataset (see e.g. Cca1 in Table S2), it is not particularly meaningful to only select the slightly best model; instead we would like to measure how well each model is supported relative to all others. This is what w_i does: it attributes a score to each model, reflecting the relative support the model offers to the data, compared to other models.

Post-hoc analysis We computed the posterior distributions of the selection gradients β_t using the HMC samples of all parameters involved, to propagate uncertainty in these estimates toward the β_t estimates. In order to do that while accounting for uncertainty in estimating $\bar{z}_t$ for models with an optimum (see Equation 2), we implemented a Monte Carlo sampling of the mean phenotype in each year, assuming a normal sampling distribution of the mean. We thus used the Monte Carlo and HMC samples of $\bar{z}_t$, θ_t and ω^2 to propagate uncertainty in estimates of β_t. We then directly used estimates of β_t to compute the mean selection gradient $E(\beta)$ and its standard deviation over the years σ_β. Note that this strategy will cause a slight regression toward the mean, and thus a slight underestimation of σ_β in general, but this is conservative with respect to the estimation of the prevalence and magnitude of fluctuating selection.

In order to obtain "meta-estimates" (i.e. robust overall estimates across all datasets, accounting for different uncertainties between datasets), we generated 100 tables (each composed of one row for each dataset), drawing from the posterior samples of $E(\theta)$, σ_θ, $E(\beta)$, σ_β and ω. We used the multiple imputation framework of the R package brms (77) to perform a mixed model analysis of each of these parameters using the taxon (bird or mammal) as a fixed effect and species and population as random effects. We used the taxon-level intercepts of such models as the meta-estimates, and report their posterior median and 95% credible interval. For $E(\theta)$, σ_θ and ω, we only used datasets with a majority statistical support for optimum models, compared to directional models.

To study the influence of phenotype optimum tracking by plastic responses at the individual level, we selected individuals that reproduced in two consecutive years, and computed the difference in average phenology between years in this subset (again, using Monte Carlo simulations to account for uncertainty thereafter). We only retained datasets with at least five individuals in common between consecutive years, for at least 10 years in total, and with a majority statistical support for an optimum. Although proper measurement of phenotypic plasticity requires data about an environmental cue that induces the plastic response, the phenotypic change caused by plasticity (i.e. the plastic response) can be inferred accurately without this information provided that other processes such as ontogeny, habitat choice or senescence, can be ignored. This assumption is generally a good approximation for phenological traits, and was used for instance by (78) to estimate selection on plasticity, even though there is some evidence for senescence of reproductive phenology and its plasticity in the wild ((79) for an example on blue tits). We then computed the correlation between plastic changes in mean individual phenotype and changes in optimum phenotype across years, still accounting for uncertainty: to test for the significance of an overall trend in these correlations, we sampled Monte Carlo and HMC iterations amounting to the sample size of each dataset, and did so 100 times. We then inferred the meta-estimate of the correlation using a mixed model in brms, as described above, using taxon as a fixed effect and study ID as a random effect.

Data availability Estimates, code and data to reproduce the analysis can be found online at: https://github.com/devillemereuil/MetaFluctSel.

1. P Inchausti, J Halley, The long-term temporal variability and spectral colour of animal populations. *Evol. Ecol. Res.* **4**, 1033–1048 (2002).
2. PR Grant, BR Grant, Unpredictable evolution in a 30-year study of Darwin's finches. *Science* **296**, 707–711 (2002).
3. R Lande, PoBS Engen, S Engen, BE Sæther, PoPEBE Saether, *Stochastic Population Dynamics in Ecology and Conservation.* (Oxford University Press), (2003).
4. DA Vasseur, P Yodzis, The color of environmental noise. *Ecology* **85**, 1146–1152 (2004).
5. MR Robinson, JG Pilkington, TH Clutton-Brock, JM Pemberton, LEB Kruuk, Environmental heterogeneity generates fluctuating selection on a secondary sexual trait. *Curr. Biol.* **18**, 751–757 (2008).
6. G Bell, Fluctuating selection: The perpetual renewal of adaptation in variable environments. *Philos. Trans. R. Soc. B Biol. Sci.* **365**, 87–97 (2010).
7. TML Wigley, RL Smith, BD Santer, Anthropogenic influence on the autocorrelation structure of hemispheric-mean temperatures. *Science* **282**, 1676–1679 (1998).
8. GJ Boer, Changes in interannual variability and decadal potential predictability under global warming. *J. Clim.* **22**, 3098–3109 (2009).
9. J Felsenstein, The theoretical population genetics of variable selection and migration. *Annu. Rev. Genet.* **10**, 253–280 (1976).
10. PW Hedrick, Genetic variation in a heterogeneous environment. I. Temporal heterogeneity and the absolute dominance model. *Genetics* **78**, 757–770 (1974).
11. JJ Bull, Evolution of phenotypic variance. *Evolution* **41**, 303–315 (1987).
12. J Tufto, Genetic evolution, plasticity, and bet-hedging as adaptive responses to temporally autocorrelated fluctuating selection: A quantitative genetic model. *Evolution* **69**, 2034–2049 (2015).
13. AG Jones, SJ Arnold, R Bürger, The mutation matrix and the evolution of evolvability. *Evolution* **61**, 727–745 (2007).

14. B Charlesworth, Directional selection and the evolution of sex and recombination. *Genet. Res.* **61**, 205–224 (1993).

15. R Bürger, Evolution of genetic variability and the advantage of sex and recombination in changing environments. *Genetics* **153**, 1055–1069 (1999).

16. S Gavrilets, SM Scheiner, The genetics of phenotypic plasticity. VI. Theoretical predictions for directional selection. *J. Evol. Biol.* **6**, 49–68 (1993).

17. R Lande, Adaptation to an extraordinary environment by evolution of phenotypic plasticity and genetic assimilation. *J. Evol. Biol.* **22**, 1435–1446 (2009).

18. CA Botero, FJ Weissing, J Wright, DR Rubenstein, Evolutionary tipping points in the capacity to adapt to environmental change. *Proc. Natl. Acad. Sci.* **112**, 184–189 (2015).

19. J Maynard Smith, What determines the rate of evolution? *The Am. Nat.* **110**, 331–338 (1976).

20. M Lynch, R Lande, Evolution and extinction in response to environmental-change in *Workshop on Biotic Interactions and Global Change*, eds. PM Kareiva, JG Kingsolver, RB Huey. (Sinauer Associates, Sunderland), (1993).

21. R Lande, S Shannon, The role of genetic variation in adaptation and population persistence in a changing environment. *Evolution* **50**, 434–437 (1996).

22. LM Chevin, O Cotto, J Ashander, Stochastic evolutionary demography under a fluctuating optimum phenotype. *The Am. Nat.* **190**, 786–802 (2017).

23. AG McAdam, S Boutin, B Dantzer, JE Lane, Seed masting causes fluctuations in optimum litter size and lag load in a seed predator. *The Am. Nat.* **194**, 574–589 (2019).

24. PD Gingerich, Rates of evolution: Effects of time and temporal scaling. *Science* **222**, 159–161 (1983).

25. S Estes, SJ Arnold, Resolving the paradox of stasis: Models with stabilizing selection explain evolutionary divergence on all timescales. *The Am. Nat.* **169**, 227–244 (2007).

26. JC Uyeda, TF Hansen, SJ Arnold, J Pienaar, The million-year wait for macroevolutionary bursts. *PNAS* **108**, 15908–15913 (2011).

27. M Kopp, S Matuszewski, Rapid evolution of quantitative traits: Theoretical perspectives. *Evol Appl* **7**, 169–191 (2014).

28. TE Reed, RS Waples, DE Schindler, JJ Hard, MT Kinnison, Phenotypic plasticity and population viability: The importance of environmental predictability. *Proc. Royal Soc. B: Biol. Sci.* **277**, 3391–3400 (2010).

29. LM Chevin, BC Haller, The temporal distribution of directional gradients under selection for an optimum. *Evolution* **68**, 3381–3394 (2014).

30. AM Siepielski, JD DiBattista, SM Carlson, It's about time: The temporal dynamics of phenotypic selection in the wild. *Ecol. Lett.* **12**, 1261–1276 (2009).

31. MB Morrissey, JD Hadfield, Directional selection in temporally replicated studies is remarkably consistent. *Evolution* **66**, 435–442 (2012).

32. C Parmesan, G Yohe, A globally coherent fingerprint of climate change impacts across natural systems. *Nature* **421**, 37–42 (2003).

33. MB Davis, RG Shaw, JR Etterson, Evolutionary responses to changing climate. *Ecology* **86**, 1704–1714 (2005).

34. C Parmesan, Ecological and evolutionary responses to recent climate change. *Annu. Rev. Ecol. Evol. Syst.* **37**, 637–669 (2006).

35. V Radchuk, et al., Adaptive responses of animals to climate change are most likely insufficient. *Nat Commun* **10**, 1–14 (2019).

36. CJ Tansey, JD Hadfield, AB Phillimore, Estimating the ability of plants to plastically track temperature-mediated shifts in the spring phenological optimum. *Glob. Chang. Biol.* **23**, 3321–3334 (2017).

37. JJC Ramakers, P Gienapp, ME Visser, Phenological mismatch drives selection on elevation, but not on slope, of breeding time plasticity in a wild songbird. *Evolution* **73**, 175–187 (2019).

38. LM Chevin, ME Visser, J Tufto, Estimating the variation, autocorrelation, and environmental sensitivity of phenotypic selection. *Evolution* **69**, 2319–2332 (2015).

39. M Gamelon, et al., Environmental drivers of varying selective optima in a small passerine: A multivariate, multiepisodic approach. *Evolution* **72**, 2325–2342 (2018).

40. M Morrissey, IBJ Goudie, Analytical results for directional and quadratic selection gradients for log-linear models of fitness functions. *bioRxiv*, 040618 (2016).

41. R Lande, SJ Arnold, The measurement of selection on correlated characters. *Evolution* **37**, 1210–1226 (1983).

42. JG Kingsolver, et al., The strength of phenotypic selection in natural populations. *The Am. Nat.* **157**, 245–261 (2001).

43. HE Hoekstra, et al., Strength and tempo of directional selection in the wild. *PNAS* **98**, 9157–9160 (2001).

44. R Lande, Natural selection and random genetic drift in phenotypic evolution. *Evolution* **30**, 314–334 (1976).

45. BDH Latter, Selection in finite populations with multiple alleles. II. Centripetal selection, mutation, and isoallelic variation. *Genetics* **66**, 165–186 (1970).

46. R Bürger, *The Mathematical Theory of Selection, Recombination, and Mutation.* (John Wiley & Sons, Chichester), (2000).

47. A Vehtari, A Gelman, J Gabry, Practical Bayesian model evaluation using Leave-One-Out cross-validation and WAIC. *Stat Comput.* **27**, 1413–1432 (2017).

48. KP Burnham, DR Anderson, Multimodel inference understanding AIC and BIC in model selection. *Sociol. Methods & Res.* **33**, 261–304 (2004).

49. T Johnson, N Barton, Theoretical models of selection and mutation on quantitative traits. *Philos. Transactions Royal Soc. B: Biol. Sci.* **360**, 1411–1425 (2005).

50. J Janzen, HS Stern, Logistic regression for empirical studies of multivariate selection. *Evolution* **52**, 1564–1571 (1998).

51. A Charmantier, et al., Adaptive phenotypic plasticity in response to climate change in a wild bird population. *Science* **320**, 800–803 (2008).

52. ME Visser, SP Caro, K van Oers, SV Schaper, B Helm, Phenology, seasonal timing and circannual rhythms: Towards a unified framework. *Philos. Transactions Royal Soc. B: Biol. Sci.* **365**, 3113–3127 (2010).

53. A Van Noordwijk, R McCleery, C Perrins, Selection for the timing of great tit breeding in relation to caterpillar growth and temperature. *J. Anim. Ecol.* **64**, 451–458 (1995).

54. ME Visser, AJ van Noordwijk, JM Tinbergen, CM Lessells, Warmer springs lead to mistimed reproduction in great tits (Parus major). *Proc. R. Soc. Lond. B Biol. Sci.* **265**, 1867–1870 (1998).

55. BC Sheldon, LEB Kruuk, J Merilä, Natural selection and inheritance of breeding time and clutch size in the collared flycatcher. *Evolution* **57**, 406–420 (2003).

56. P Gienapp, E Postma, ME Visser, Why breeding time has not responded to selection for earlier breeding in a songbird population. *Evolution* **60**, 2381–2388 (2006).

57. C Teplitsky, JA Mills, JW Yarrall, J Merilä, Indirect genetic effects in a sex-limited trait: The case of breeding time in red-billed gulls. *J. Evol. Biol.* **23**, 935–944 (2010).

58. T Pärt, J Knape, M Low, M Öberg, D Arlt, Disentangling the effects of date, individual, and territory quality on the seasonal decline in fitness. *Ecology* **98**, 2102–2110 (2017).

59. PM Sirkiä, et al., Climate-driven build-up of temporal isolation within a recently formed avian hybrid zone. *Evolution* **72**, 363–374 (2018).

60. P de Villemereuil, A Rutschmann, JG Ewen, AW Santure, P Brekke, Can threatened species adapt in a restored habitat? No expected evolutionary response in lay date for the New Zealand hihi. *Evol. Appl.* **12**, 482–497 (2019).

61. JE Lane, LEB Kruuk, A Charmantier, JO Murie, FS Dobson, Delayed phenology and reduced fitness associated with climate change in a wild hibernator. *Nature* **489**, 554–557 (2012).

62. H Holand, et al., Stabilizing selection and adaptive evolution in a combination of two traits in an arctic ungulate. *Evolution* **74**, 103–115 (2020).

63. J Merilä, B Sheldon, L Kruuk, Explaining stasis: Microevolutionary studies in natural populations. *Genetica* **112**, 199–222 (2001).

64. T Price, M Kirkpatrick, S Arnold, Directional selection and the evolution of breeding date in birds. *Science* **240**, 798–799 (1988).

65. J Johansson, HG Smith, N Jonzén, Adaptation of reproductive phenology to climate change with ecological feedback via dominance hierarchies. *J. Anim. Ecol.* **83**, 440–449 (2014).

66. D Schluter, TD Price, L Rowe, PR Grant, Conflicting selection pressures and life history trade-offs. *Proc. Royal Soc. London. Ser. B: Biol. Sci.* **246**, 11–17 (1991).

67. P Gienapp, TE Reed, ME Visser, Why climate change will invariably alter selection pressures on phenology. *Proc. Royal Soc. B: Biol. Sci.* **281**, 20141611 (2014).

68. S Boutin, et al., Anticipatory reproduction and population growth in seed predators. *Science* **314**, 1928–1930 (2006).

69. B Dantzer, et al., Density triggers maternal hormones that increase adaptive offspring growth in a wild mammal. *Science* **340**, 1215–1217 (2013).

70. ME Visser, LJM Holleman, P Gienapp, Shifts in caterpillar biomass phenology due to climate change and its impact on the breeding biology of an insectivorous bird. *Oecologia* **147**, 164–172 (2006).

71. S Bonamour, LM Chevin, A Charmantier, C Teplitsky, Phenotypic plasticity in response to climate change: The importance of cue variation. *Phil. Trans. R. Soc. B* **374**, 20180178 (2019).

72. LD Bailey, et al., Songbird populations most exposed to climate change tend to be less climate sensitive. *bioRxiv* (2020).

73. ME Visser, Keeping up with a warming world; assessing the rate of adaptation to climate change. *Proc. Royal Soc. B: Biol. Sci.* **275**, 649–659 (2008).

74. LM Chevin, R Lande, Evolution of environmental cues for phenotypic plasticity. *Evolution* **69**, 2767–2775 (2015).

75. MD Hoffman, A Gelman, The No-U-Turn Sampler: Adaptively Setting Path Lengths in Hamiltonian Monte Carlo. *J. Mach. Learn. Res.* **15**, 1593–1623 (2014).

76. A Vehtari, A Gelman, D Simpson, B Carpenter, PC Bürkner, Rank-normalization, folding, and localization: An improved R for assessing convergence of MCMC. *ArXiv190308008 Stat* (2019).

77. PC Bürkner, Advanced bayesian multilevel modeling with the R package brms. *ArXiv170511123 Stat* (2017).

78. JE Brommer, E Kluen, Exploring the genetics of nestling personality traits in a wild passerine bird: Testing the phenotypic gambit. *Ecol. Evol.* **2**, 3032–3044 (2012).

79. S Bonamour, LM Chevin, D Réale, C Teplitsky, A Charmantier, Age-dependent phenological plasticity in a wild bird. *J. Anim. Ecol.* (2020).